Foothold Placement Planning with a Hexapod Crawling Robot

Petr Čížek Diar Masri Jan Faigl

***Abstract*— In this work, we concern the problem of motion planning for a hexapod walking robot crawling in a semi-structured environment where a precise foot-tip positioning is necessary. We propose pipelined approach utilizing an RGB-D camera to perceive and map the forthcoming terrain in 2.5 D which is then processed for available foot-tip positions. The robot motion control is based on sampling-based planning to determine the most suitable leg supporting configurations for the individual body positions in the created terrain map. The individual body positions are connected into a roadmap with taking into account a feasibility of the robot transition between the individual configurations. The resulting trajectory is then planned in the created roadmap using a standard A* planner. The proposed method has been experimentally evaluated in the on-line and onboard setup with a real hexapod crawling robot. The herein reported results support feasibility of the proposed approach for a precise motion planning of small hexapod crawling robot in a semi-structured environment.**

I. Introduction

Stepping stones are a neat example of a semi-structured terrain impassable by wheeled or tracked robots but still imposing a great challenge to legged robots. Such a scenario requires a full deliberative control and individual foot-tip positions of each leg need to be planned in advance. In the legged robot locomotion, the obstacles can be overcome through reactive control and reflexes (e.g., [1], [2]), or a mechatronic design of the robot (e.g., [3]) can substantially improve the ability of the robot to overcome rough terrains; however, for more complex environments containing large gaps or stairs, such solutions quickly reach their limits.

Therefore motion planning has to be incorporated into the locomotion control to take advantage of the situation awareness build by the robot itself in a form of a local map of the robot surroundings. In this work, we propose an integrated approach for a deliberative control of a hexapod walking robot to plan a trajectory with individual footholds to safely navigate the robot from a start location to the desired goal location through a previously unknown terrain.

In particular, we concern the problem of locomotion planning with a low-cost hexapod walking robot with limited sensory equipment and using only the onboard computational power. The essential stages of the local map building, localization, and foothold planning are connected in a simple yet efficient integrated motion planning approach which employs a probabilistic roadmap to provide a feasible path regarding the local footsteps and transitions between the individual configurations. Moreover, we emphasize a deployment of the system in fully autonomous missions where all calculations are performed on-line onboard of the mobile robot. The proposed approach has been experimentally verified with a real robot in scenarios with foothold placement on stepping stones, see Fig. 1. The experimental results show that the approach enables the robot to overcome obstacles that are impassable by neither regular nor adaptive motion gait [2].

Authors are with Dept. of Computer Science, Faculty of Electrical Engineering, Czech Technical University in Prague, Czech Republic {cizekpe6|masridia|faiglj}@fel.cvut.cz

The presented work has been supported by the Czech Science Foundation (GAČR) under research project No. 15-09600Y.

Fig. 1. An experimental setup assembling the stepping stones

The reminder of the paper is organized as follows. Section II lists the related work on the deliberative control of the hexapod walking robots. The proposed foothold planner is thoroughly described in Section III and evaluation results with the real walking robot are reported in Section IV. The concluding remarks are dedicated to Section V.

II. Related work

Motion planning in rough terrains and foothold selection are widely studied problems within the context of legged robots. A high number of degrees of freedom (DOF) gives the legged robots great options for motion planning and foothold selection in rough terrain. However, it is also the main difficulty as the design of an efficient locomotion control for a multi-legged robot is a challenging problem.

In complex terrains, it is suitable to calculate individual leg footholds and transitions between them directly, and thus provide safe robot control. A local map of the environment is a necessary input for such a planning process. The individual footholds can be then selected with respect to the expected traversability of the particular areas of the mapped environment. Binary [4] or more elaborate traversability assessment based on geometric features of the environment have been presented in the literature. These features include calculated properties like height and average slopes of the mapped environment [5]–[7], or template matching using adaptive decision surfaces [8], [9] or terrain templates learned from

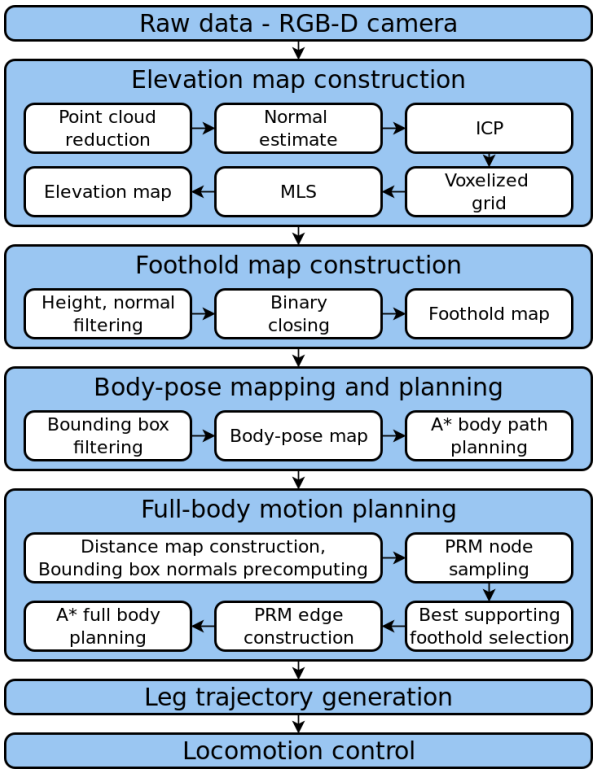

Fig. 2. An overview of the proposed controller

guided examples [10].

A number of approaches use a decomposition of the motion planning into coarse planning that finds a collision-free trajectory for the body of the robot that is followed by planning of individual footsteps in a greedy way. Popular motion planners for the coarse planning are based on A* [11] and its anytime-repairing variants [7], [10]. Besides, variants of the Rapidly growing Random Tree (RRT) algorithms have been also used, e.g., the RRT-connect used in [4] for non-gaited locomotion control which is more versatile but also a much more computationally demanding. A combination of the RRT with A* is presented in [9] to avoid unnecessary growth of the motion plan tree.

The herein presented approach combines the adaptability of the integrated approach presented in [9] with foothold selection rules most similar to the one used in [7]. In comparison to [9], we use a probabilistic roadmap [12] for the full-body motion planning accelerated by coarse body-path planning to avoid random sampling of unrelated areas of the map. The roadmap ensures a feasible path is found both in terms of the local footsteps and transitions between individual configurations of the robot given by the utilized foothold selection rule.

III. Proposed solution

Individual phases of the proposed deliberative foot-tip planning method are depicted in Fig. 2. The operation of the proposed locomotion control can be briefly described as follows. First, the forthcoming terrain is perceived by the RGB-D camera creating a 2.5 D elevation map of the environment to localize the robot with respect to the obstacles. The map is then quickly evaluated for passable and impassable areas based on surface normals and roughness of the terrain, which provides rough estimation of the traversable areas. An A* planner is then used to verify reachability of the desired goal location of the robot. Afterwards, the best supporting leg configurations are assessed for random-sampled body poses in the map. These poses are then connected into a roadmap [12] based on feasibility of the transition between individual leg configurations. Then, the A* planner is used to find a shortest path from the start location to the goal location in the created roadmap. The path is then refined to avoid collision of the leg with the terrain during the transition phase of an individual step and it is executed by the robot. A detailed description of the proposed pipelined approach is presented in the following paragraphs.

A. Elevation map construction

Despite advanced algorithms of simultaneous localization and mapping (SLAM) can be used for mapping the forthcoming terrain, e.g., like in [9], we utilize a minimalistic approach to localize the robot and create a map of the robot surroundings because of limited onboard computational resources.

First, the point cloud C_s obtained by the RGB-D camera is reduced using a bounding box to incorporate only the measurements in the vicinity of the robot given by the pre-defined threshold. A transformation is also applied to compensate for the tilt of the RGB-D sensor as the approach assumes camera axis to be parallel to the terrain being traversed. Afterwards, the surface normals are calculated for each point $p \in C_s$ as

$$\overrightarrow{n_p} = \overrightarrow{v_{1p}} \times \overrightarrow{v_{2p}}, \tag{1}$$

where $\overrightarrow{v_{1p}}$ and $\overrightarrow{v_{2p}}$ are the vectors between point p and its first and second nearest neighbor.

After that, the iterative closest point (ICP) algorithm [13] is applied to find the transformation that minimizes the mean squared error between the current point cloud C_s and the target global map C_t. The ICP algorithm is initialized with the 6-DOF position given by the legged odometry. The point to surface matching is applied, and once the transformation is estimated, the target point cloud C_t is updated by merging with the point cloud C_s, and the localization of the robot is refined.

The resulting point cloud C_t is then downsampled in voxels of size $(0.01 \times 0.01 \times 0.01)$ metres to limit the memory demands of the algorithm. The points falling in each voxel are represented with their centroid. Afterwards, the moving least square algorithm [14] is employed to filter a possible noise in the voxel grid.

Finally, the elevation map is created as a grid map covering the considered area in the close vicinity of the robot, see Fig. 3a. Each grid cell represents a squared area with the side 0.01 m corresponding to the dimensions of the voxel grid and stores the maximum measured terrain height z together with the surface normal $\overrightarrow{n}$.

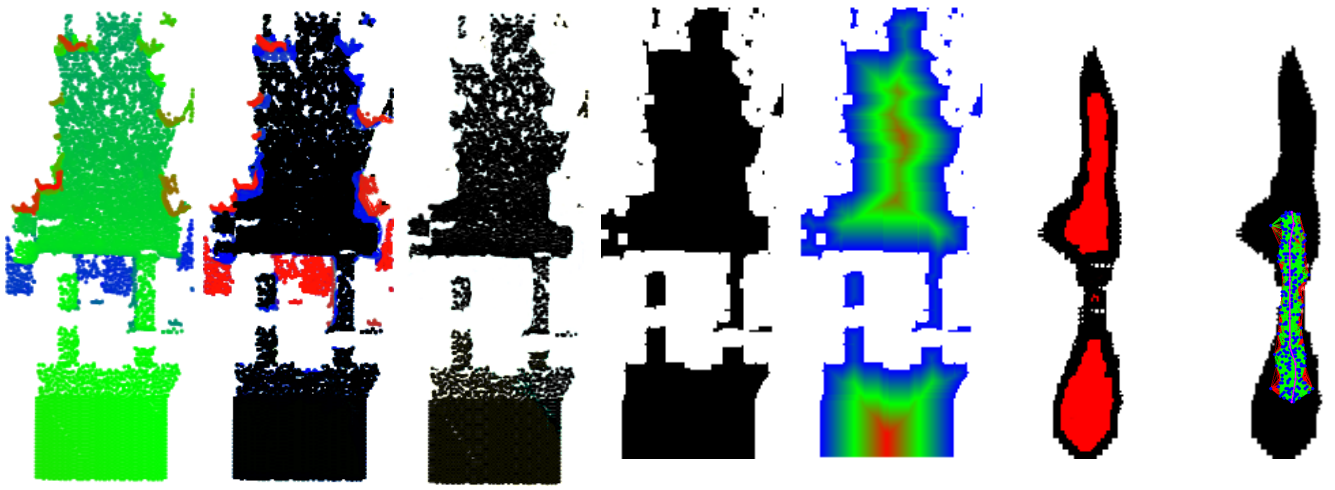

(a) (b) (c) (d) (e) (f) (g)

Fig. 3. Individual maps of the scenario depicted in Fig 1. (a) Elevation map, (b) Filtered areas, (c) Accessible areas, (d) Foothold map, (e) Distance map, (f) Body-pose map, (g) Probabilistic roadmap.

B. Foothold map construction

The traversability assessment processes the elevation map (Fig. 3a) from the previous step as follows. First, the elevation map is evaluated for accessible and inaccessible regions. Fig. 4 shows the ideal operating space of the robot leg given by kinematics of our particular hexapod robot. In general, the maximum and minimum step height are given as $s_{max} - s_{min}$ from Fig. 4; however, in the presented work we do not concern any footholds higher than the body level. Therefore we use a constant threshold of $[-(s_{max} - s_{min})/2, 0]$ to evaluate accessible and inaccessible areas.

Note, a planar motion of the body with a fixed horizontal orientation is considered in the presented approach. This simplification helps to quickly evaluate the potential footholds but deny the robot to plan a path in a terrain with slopes or high steps.

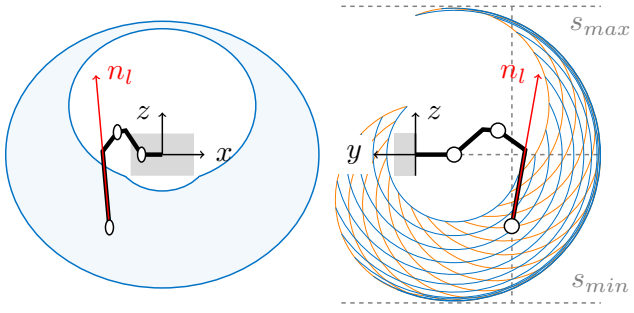

Fig. 4. Ideal working space of a hexapod leg

After filtering the unreachable areas, locations directly neighboring them are also filtered out by inflating the found obstacles using operation of binary dilation with predefined structure element with the size of the leg endpoint. Unreachable locations are depicted in the red color in Fig. 3b.

Then, locations with undesirable normals are also filtered out, as we are looking for locations with the maximal support. When considering a planar motion, the maximal support to the robot stable position is provided by the areas with normals perpendicular to the horizontal plane, and thus points with normals with the deviation

$$\psi = \cos^{-1}\left(\frac{\overrightarrow{n} \cdot [0,\, 0,\, 1]}{|\overrightarrow{n}|}\right), \tag{2}$$

greater than $\pi/4$ from the vertical direction are considered as unstable and marked as inaccessible (depicted in the blue color in Fig. 3b). The constant of $\pi/4$ has been chosen experimentally as the utmost slope the robot can walk on without a slippage.

The result of the described processing is a binary map as depicted in Fig. 3c. This map can be used with our foothold planning algorithm; however, as there are still a number of faulty and missing measurements in the map, a binary closing operation is performed on the map to remove smaller gaps and create the final foothold map, see Fig. 3d. The operation is justified by an assumption of smooth terrain, mechanical constitution, and precision of the foot placement. As the leg endpoint is larger than the utilized grid resolution, it is possible to perform the binary closing operation with structure element of the leg's endpoint size to neglect smaller holes in the real terrain, while the larger ones remain.

C. Body-pose mapping and planning

The above described foothold map construction evaluates the map for possible locations where a foot-tip can be placed; however, to plan the full-body motion, it is necessary to evaluate the possible positions for the robot body in a task space before establishing the joint space plan. The robot is represented by its center of gravity and position of the default footholds in the task space as it is visualized in Fig. 5. Further, a foothold search area is established around each default foot-tip position as a square bounding box (see Fig. 5) which is rather a simplification of a complex working space

of the robot leg depicted in Fig. 4; however, at this stage, it is fully sufficient for the verification of the overall accessibility of the goal location and estimation of the body-pose map. Its usage in a full-body motion planning is further elaborated in Section III-D. The idea is based on [7] which originates in [5].

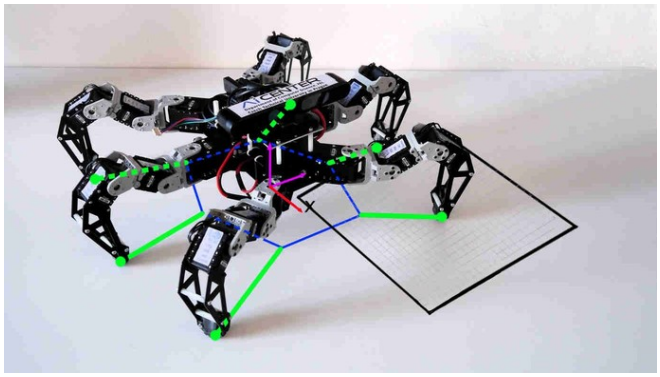

Fig. 5. The used hexapod walking robot with illustrated center of gravity and default foot tip positions projected on the ground plane together with the foothold search area (bounding box) of front-left leg

The body-pose map (Fig. 3f) is constructed as follows. For each body position in the map, the feasibility of that position for full-body planning is established by counting the number of accessible positions in a foothold map given the square bounding box of each leg. The leg is considered feasible for planning if there are at least c accessible positions in its bounding box. The given body-pose associated with the map position is considered feasible if all the robot legs support its feasibility. Note, c is set experimentally to a relatively low value to filter only obviously poor body-positions. Setting c too high may result in a sparse body-pose map and consequently planning failure as it is visualized in the red color in Fig. 3f.

The reachability of the goal position is verified using the A* planner with the Euclidean distance as the heuristics. If the planning fails, the goal is considered unreachable.

D. Full-body motion planning

The proposed motion planning approach is based on a construction of the probabilistic roadmap [12] represented as a graph $G(V, E)$, where each node $q \in V$ represents the robot configuration and an edge $e \in E$ connecting two nodes $e = (q_a, q_b), q_a, q_b \in V$ represents a feasible motion between the nodes. The planning is performed as follows.

First, random positions around the estimated path are sampled in the body-pose map to form the roadmap (the blue dots in Fig. 3g), such a graph is then searched for the shortest trajectory. For each $q \in V$, the best supporting foothold for each leg is assessed in its bounding box. A value of the sc score function is assigned to every position in the leg's bounding box that evaluates its robustness and suitability by the kinematic margin sc_{kin}, position margin sc_{pos}, and robustness margin sc_{sup} as:

$$sc = sc_{kin} \cdot sc_{pos} \cdot sc_{sup}, \tag{3}$$

where each score is normalized to a value between 0 and 1.

The kinematic margin represents the angle under which the leg is standing on the surface, which is given by the surface normal and the direction vector n_l of the leg visualized in Fig. 4. To speed-up the computation, the evaluation uses a pre-computed look-up table of n_l vectors in the cube with the outline of the bounding box and the height of $[-(s_{max} - s_{min})/2,\ 0]$ with the same resolution as the voxel grid used in the foothold map build process. The points in the cube that lie outside the working space are assessed the null value. As all the surface points with normals greater than $\pi/4$ have been filtered out in the foothold map creation step, the maximum normal difference at the given bounding box is less than π which serves as the normalization constant.

The position margin stands for the feasibility of the foothold, which is given by the working space of the robot leg, which is also easily evaluated using the look-up table, and the distance of the leg's endpoint to the robot trunk as a higher distance is better for the stability of the robot.

Finally, the robustness margin evaluates the expected robustness of the foothold given by the distance map (Fig. 3e) which evaluates the distance from the closest obstacle. The distance map is computed using the distance transform with the Manhattan distance and thresholded to allow normalization of sc_{sup}. The threshold is set to three times the size of leg's endpoint; hence, any footholds further from obstacles than that are considered equally good, only close-to-edge footholds are penalized.

The best supporting foothold is given as the one with the highest score. Furthermore, the scores for individual legs given particular node q sums up to provide a global score for the given node. Unfortunately, there is no mechanism implemented to resolve deconfliction of possibly interfering footholds at this point.

When all the nodes in the roadmap are assigned with a score, edges are established by the distance estimation between the adjacent nodes and feasibility of the transition between them. The distance estimation serves as a rapid rejection method that rejects any edge connecting two robot poses with a distance longer than e_{max}. The feasibility test consists of the evaluation of the robot full-body pose along the edge. In our experimental evaluation, we have used the pentapod motion gait which defines the pattern in which the individual legs moves. Thus, the movement of the body is uniformly discretized to 5 separate poses as it is visualized in Fig. 6. A score is assigned to each intermediate configuration according to Eq. 3 in the same way described above. The resulting edge score sc_e is given as the sum of the intermediate scores and it is normalized to the range $[0, 1]$ given the maximum reachable score. Moreover, if an edge violates the position margin, i.e., the foot cannot reach the goal configuration, the edge is rejected.

Finally, the A* planner is used to plan the path between the start and goal locations in the created roadmap. Euclidean distance to the goal weighted by the complementary edge score $(1 - sc_e)$ is used as the heuristic function in the planner. The result of the planning is shown in Fig. 3g where the blue dots represent nodes, green and red lines represent feasible

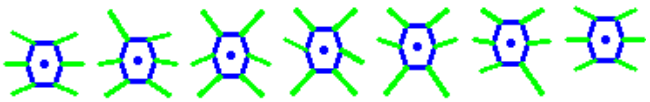

Fig. 6. Discretization of the transition between two configurations. One leg swings at a time according to pentapod gait.

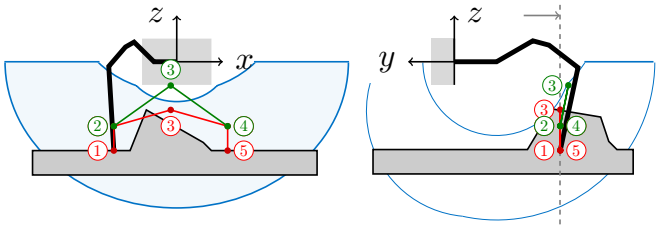

Fig. 7. Leg trajectory generation. Each step is discretized into 5 configurations. The terrain is represented by black, the colliding default trajectory is in red and the refined trajectory is in green.

and infeasible transitions, respectively, and the magenta line shows the planned trajectory.

E. Leg trajectory generation

A transition plan for each leg is established for a collision evasion, whenever a path in the roadmap is found. The main idea of the trajectory generation is to provide a detail sequence of the intermediate steps T of the moving leg to avoid possible collision with the underlying surface during the swing phase. Hence, the swing motion of the leg from one foothold location ① to a new one ⑤ is split into 3 intermediate configurations ②③④ as it is shown in Fig. 7.

Bresenham algorithm is used for the projection of the leg trajectory into the elevation map to evade collision with the terrain. If the distance of the leg's endpoint during the transition between states ②,③ and ④ is beneath the allowed level of 2 cm, the nearest higher reachable endpoint position in the leg operational space is selected. If any configuration falls outside the vertical admissible working space of the leg as depicted in Fig. 7, where configuration ③ falls outside the reachable area, the next closest admissible configuration is selected according to the Euclidean distance.

F. Locomotion control

The resulting path given by the full-body motion planner together with the refined collision-free trajectories for each leg are fed into the locomotion controller. The locomotion controller converts the plan to the joint space using inverse kinematics and executes the trajectory by the direct servo control. Note, there is currently no feedback mechanism that would recognize missing foot-hold, collision with obstacle or soft terrain. In the near future, we aim to address this drawback by incorporating mechanisms of adaptive motion gait [2] into the execution of the plan.

IV. Experimental evaluation

The proposed foot-tip planning and locomotion control mechanism have been experimentally verified with a hexapod walking robot in a scenario that requires a precise foothold planning on stepping stones. The experimental deployment is described in the following subsections.

A. Hexapod walking platform

The utilized crawling platform is based on an electrically actuated low-cost hexapod robot. It features six legs, each with 3 joints attached to the trunk which hosts the electronics and sensory equipment. In the default configuration, the robot dimensions are approx. 45×40 cm. The RGB-D ASUS Xtion Pro Live camera has been utilized for the terrain perception. The algorithm has run on-line onboard of the Odroid U3 embedded computer with the 1.7 GHz ARM Cortex A9 quad-core processor (Samsung Exynos4412) and 2GB RAM. Note, the cable visible in the photos has been used only for telemetry transmission and all computations have been performed onboard.

B. Experimental setup

The experimental setup is depicted in Fig. 1. It consists of two 160 cm long desks separated by a 60 cm gap with sparse stepping stones formed by wooden cubes of size 10×10 cm. The height of the traversable surface above ground is 12 cm. For each of the performed experiments, the robot is given the $\delta x, \delta y$-coordinates of the goal location and it is requested to plan the trajectory and follow it. The whole scenario measures 3.8 m and the robot is requested to traverse 2.4 m distance of it (1.0 m in front of the obstacle, 0.6 m stepping stones, 0.8 m behind obstacle) with new RGB-D data fetching and replanning each 0.8 m. The map is sampled for 250 nodes to construct the roadmap with maximum pose-to-pose distance $e_{max} = 20$ cm. The bounding box for the foothold planning around the foot-tip is 40×40 cm large.

C. Results and discussion

Snapshots from the robot traversing the environment and visualization of the planned configuration of the robot are depicted in Fig. 9. Altogether 10 trials have been performed with the success rate of the full body planning phase 90%. In one case, the planning fails in body-pose planning phase, in each of the 9 rest cases, a feasible path from the start location to the goal location has been found. The whole planning takes approx. 9 s for the considered scenario.

However, the execution of the plan proves to be more challenging than the planning itself. Due to the low posture of the RGB-D sensor on the robot, it is necessary to perform standing maneuver to sample a sufficiently dense point cloud (see Fig. 8). Therefore we have scheduled map refinement and replanning after each 80 cm of traversed distance which has shown to be too sparse as only a small deviation in the plan execution due to joints compliance and mechanical

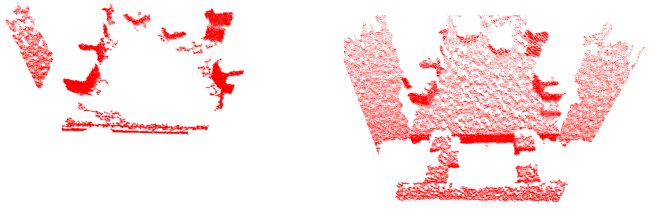

(a) (b)

Fig. 8. RGB-D perception: (a) in walking position (b) in standing position

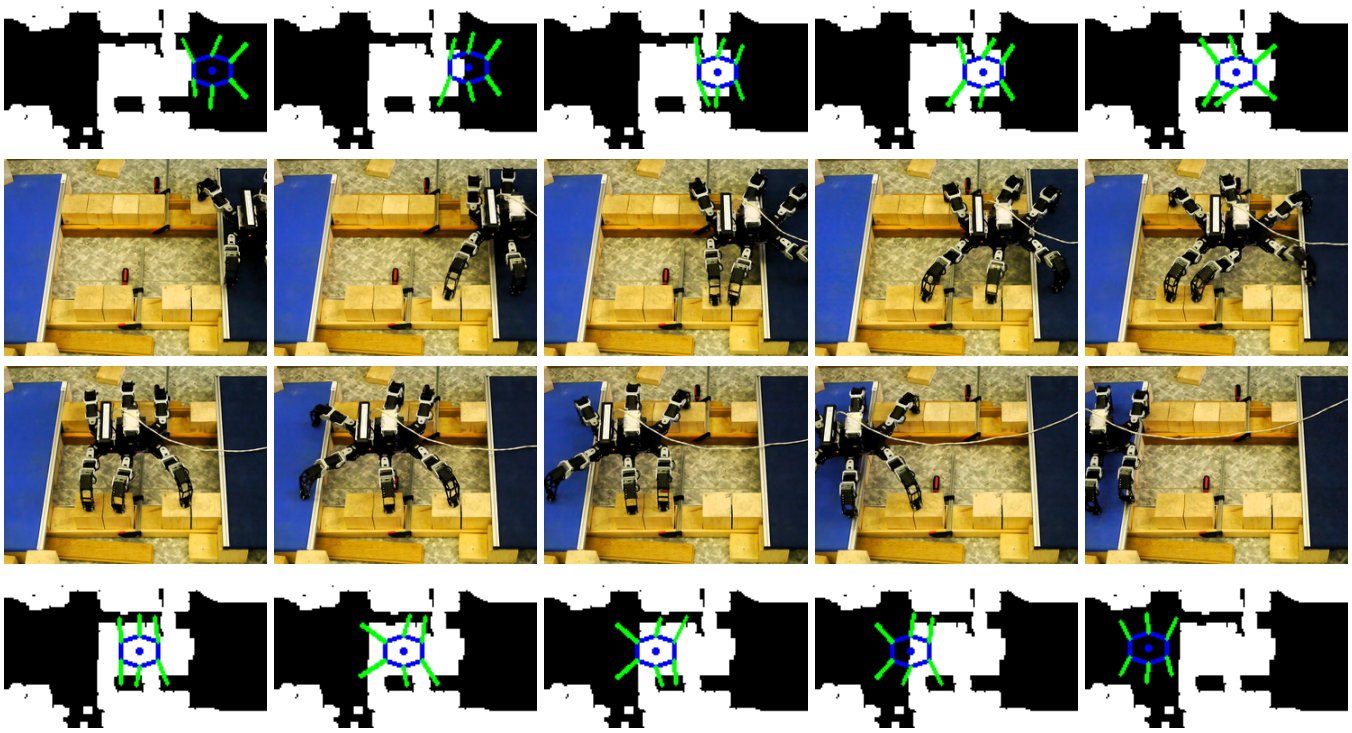

Fig. 9. Snapshots of the experimental traverse of the stepping stones scenario. For each photo there is a body-configuration established by the planner.

imperfections results in the failure of the execution. Hence, in only 5 out of the remaining 9 trials the robot has been successful in traversing the whole path.

Notice, regarding the performance of the blind crawling using regular and adaptive motion gaits [2], both these approaches were unable to traverse the experimental setup.

V. Conclusion

In this work, we propose an integrated foot-tip motion planning and control algorithm for a hexapod walking robot capable of on-line onboard performance. The proposed foothold planner has been experimentally verified in real scenarios assembling a problem of precise foothold planning on stepping stones. The experimental results support feasibility of the proposed planner to overcome semi-structured terrains impassable by regular nor adaptive blind motion gaits [2].

The robustness of the proposed minimalist solution can be further improved by using a better SLAM system and by incorporating the robot motion model for foothold planning in complex terrains as we consider several simplifications of the rather complex leg operation space. These topics are considered as a subject for the future work.

References

[1] K. S. Espenschied, R. D. Quinn, R. D. Beer, and H. J. Chiel, "Biologically based distributed control and local reflexes improve rough terrain locomotion in a hexapod robot," *Robotics and Autonomous Systems*, vol. 18, no. 1-2, pp. 59–64, 1996.

[2] J. Mrva and J. Faigl, "Tactile sensing with servo drives feedback only for blind hexapod walking robot," in *10th International Workshop on Robot Motion and Control*, 2015, pp. 240–245.

[3] U. Saranli, M. Buehler, and D. E. Koditschek, "RHex: A simple and highly mobile hexapod robot," *The International Journal of Robotics Research*, vol. 20, no. 7, pp. 616–631, 2001.

[4] N. Perrin, C. Ott, J. Englsberger, O. Stasse, F. Lamiraux, and D. G. Caldwell, "Continuous legged locomotion planning," *IEEE Transactions on Robotics*, vol. 33, no. 1, pp. 234–239, 2017.

[5] J. Z. Kolter, M. P. Rodgers, and A. Y. Ng, "A control architecture for quadruped locomotion over rough terrain," in *IEEE Int. Conf. on Robotics and Automation*, 2008, pp. 811–818.

[6] A. Stelzer, H. Hirschmüller, and M. Görner, "Stereo-vision-based navigation of a six-legged walking robot in unknown rough terrain," *The International Journal of Robotics Research*, vol. 31, no. 4, pp. 381–402, 2012.

[7] A. W. Winkler, C. Mastalli, I. Havoutis, M. Focchi, D. G. Caldwell, and C. Semini, "Planning and execution of dynamic whole-body locomotion for a hydraulic quadruped on challenging terrain," in *IEEE Int. Conf. on Robotics and Automation*, 2015, pp. 5148–5154.

[8] D. Belter and P. Skrzypczyński, "Rough terrain mapping and classification for foothold selection in a walking robot," *Journal of Field Robotics*, vol. 28, no. 4, pp. 497–528, 2011.

[9] D. Belter, P. Łabecki, and P. Skrzypczynski, "Adaptive motion planning for autonomous rough terrain traversal with a walking robot," *Journal of Field Robotics*, vol. 33, no. 3, pp. 337–370, 2015.

[10] J. Buchli, J. Pratt, N. Roy, M. Kalakrishnan, J. Buchli, P. Pastor, M. Mistry, and S. Schaal, "Learning, planning, and control for quadruped locomotion over challenging terrain," *The International Journal of Robotics Research*, vol. 30, no. 2, pp. 236–258, 2011.

[11] M. A. Arain, I. Havoutis, C. Semini, J. Buchli, and D. G. Caldwell, "A comparison of search-based planners for a legged robot," in *9th International Workshop on Robot Motion and Control*, 2013, pp. 104–109.

[12] L. E. Kavraki, P. Svestka, J. C. Latombe, and M. H. Overmars, "Probabilistic roadmaps for path planning in high-dimensional configuration spaces," *IEEE Transactions on Robotics and Automation*, vol. 12, no. 4, pp. 566–580, 1996.

[13] Z. Zhang, "Iterative point matching for registration of free-form curves and surfaces," *International Journal of Computer Vision*, vol. 13, no. 2, pp. 119–152, 1994.

[14] M. Alexa, J. Behr, D. Cohen-Or, S. Fleishman, D. Levin, and C. T. Silva, "Computing and rendering point set surfaces," *IEEE Transactions on visualization and computer graphics*, vol. 9, no. 1, pp. 3–15, 2003.